

## Electron emission in double-electron capture with simultaneous single ionization in 30-keV/u ${}^4\text{He}^{2+}$ -Ar collisions

R. T. Zhang,<sup>1,\*</sup> X. Ma,<sup>1,†</sup> S. F. Zhang,<sup>1</sup> X. L. Zhu,<sup>1</sup> W. T. Feng,<sup>1</sup> D. L. Guo,<sup>1,2</sup> Y. Gao,<sup>1,2</sup> B. Li,<sup>1</sup>  
D. B. Qian,<sup>1</sup> H. P. Liu,<sup>1</sup> S. Yan,<sup>1</sup> and P. Zhang<sup>1</sup>

<sup>1</sup>*Institute of Modern Physics, Chinese Academy of Sciences, Lanzhou 730000, China*

<sup>2</sup>*University of Chinese Academy of Sciences, Beijing 100049, China*

(Received 3 November 2013; revised manuscript received 16 January 2014; published 14 March 2014)

Electron emissions are studied for the double-electron capture with simultaneous single ionization process in 30 keV/u  $\text{He}^{2+}$ -Ar atom collision using the reaction microscope technique. Double-differential cross sections have been obtained for emission angles of  $0^\circ$ ,  $20^\circ$ ,  $45^\circ$ ,  $90^\circ$ ,  $128^\circ$ , and  $175^\circ$  and electron energies ranging from 0 to 80 eV. No cusp-shaped electrons centered at a speed equal to that of the incident projectile in the forward direction are observed, which is contrary to the earlier results [D. Fregenal, J. Fiol, G. Bernardi, S. Suarez, P. Focke, A. D. Gonzalez, A. Muthig, T. Jalowy, K. O. Groeneveld, and H. Luna, *Phys. Rev. A* **62**, 012703 (2000)]. An explanation has been provided to clarify the observed results in the current reaction channel.

DOI: [10.1103/PhysRevA.89.032708](https://doi.org/10.1103/PhysRevA.89.032708)

PACS number(s): 34.50.-s, 34.70.+e

In ion-atom collisions, the cusp-shaped peak, which appears in the energy spectrum of emitted electrons in the forward direction, has been extensively studied both experimentally and theoretically [1–7] since it was first observed by Crooks and Rudd [8]. Earlier studies primarily focused on single ionization and indicated that the Coulomb interaction between the ejected electron and the outgoing projectile played a decisive role in the formation of the cusp [9–13]. Recently, with the development of coincidence measurements and imaging techniques, considerable efforts have been dedicated to two or more electron transition processes [14,15], which include transfer ionization, in which the ionization of the target (ejection of one or more electrons) is accompanied by the transfer of an additional electron (or several electrons) from the target to the projectile. Many different electron emission mechanisms, including the role of static and dynamic electron correlations, have been confirmed in the transfer ionization involving a helium target [16–18]. However, understanding the cusp-shaped electron emissions in the transfer ionization (TI) still faces considerable challenges.

The cusp-shaped electron emission in the TI was firstly studied by Závodszky *et al.* [19] and Zhu *et al.* using structured-ion projectiles ( $\text{He}^+$ ,  $\text{O}^{7+}$ ) [20]. Later, fully stripped ions such as  $\text{H}^+$ ,  $\text{He}^{2+}$ , and  $\text{O}^{8+}$  were used to simplify comprehension [21,22]. The simplest case is the proton impact, which provides the smallest perturbation. Additionally, transfer ionization using a proton projectile leads to a neutral outgoing projectile; this addresses the problem of threshold behavior involving the short-range potential. As is commonly known, the cusp is a consequence of the long-range Coulomb interaction between the emitted electron and the outgoing

charged projectile ion and is not expected in the case of a neutral outgoing projectile [23]. However, Sarkadi *et al.* provided the first experimental evidence of cusp-shaped electron emission for the neutral outgoing projectile [24]. Subsequently, various ideas were proposed to explain the observation by Sarkadi, e.g., an exchange mechanism proposed by Salin [25], a  $\text{He}^{-**}$  nonmetastable autodetaching mechanism [26], and a final state interaction (FSI) theory proposed by Barrachina [27]. Among these models, the FSI theory was confirmed by several experiments [28–30]. Recently, Bernardi *et al.* [30] measured the cusp-shaped electron emission in the collisions between  $\text{H}^+$  and He. Their results indicated that a dipole interaction between the excited H and the emitted electron led to the cusp formation.

Now, we turn to the more complicated case of the collision of  $\text{He}^{2+}$  and argon, and focus on cusp electron emission involving a two-electron capture. In this reaction channel, Double electrons are captured into the bound state of the projectile while one target electron is simultaneously ionized into the continuum (DCI). The DCI process is described as follows:



Moretto-Capelle *et al.* [31] studied the transfer ionization in 12.5 keV/u  ${}^3\text{He}^{2+}$  collisions with argon employing a cylindrical mirror electron spectrometer and detecting coincidences between the emitted electrons and the neutral He atoms, and concluded that two electrons are mainly transferred to the ground state of He in the DCI process. Later, Fregenal *et al.* [32] observed a prominent cusp peak in the electron energy spectrum of the DCI process in the 25 keV/u  ${}^3\text{He}^{2+}$  on argon collisions.

In this study, we investigated electron emissions in the DCI process of 30 keV/u  $\text{He}^{2+}$  on argon collisions, using the reaction microscope technique and detecting triple coincidences between the outgoing projectiles, the emitted electrons, and the recoil ions. Our goal is to promote further inquiry and debate on cusp formation in the DCI process of  $\text{He}^{2+}$  collisions with argon. Double-differential cross sections (DDCSs) as a

\*r.zhang@gsi.de; present address: ExtreMe Matter Institute EMMI and Research Division, GSI Helmholtzzentrum für Schwerionenforschung, Planckstraße 1, 64291 Darmstadt, Germany and FIAS Frankfurt Institute for Advanced Studies, 60438 Frankfurt am Main, Germany.

†Corresponding author: x.ma@impcas.ac.cn

function of ejected-electron energy are obtained for different emission angles. Surprisingly, there is no cusp peak in the forward energy spectrum, which is contrary to the observation by Fregenal *et al.* [32]. Within the framework of FSI theory and the potential curve of  $\text{He}^{2+}\text{-Ar}$  [31], it is suggested that cusp-shaped electron emission is not expected in the DCI process. Consequently, we conclude that cusp-shaped electron emission cannot exist in the current DCI process.

Atomic units (a.u.) will be used throughout unless indicated otherwise.

We performed an experiment on 30 keV/u  $\text{He}^{2+}\text{-Ar}$  collisions using reaction microscope, which was mounted at the 320-kV platform for multidiscipline research with highly charged ions at the Institute of Modern Physics in Lanzhou, China. The working principles of the reaction microscope have been described in detail in Refs. [14,15,33]. Briefly, the  $\text{He}^{2+}$  ions produced in the electron cyclotron resonance ion resource (ECR) are first charge selected by an analyzing magnet and then accelerated to the desired energy when leaving the high-voltage platform. The ion beam is collimated to smaller than  $1 \times 1 \text{ mm}^2$  before entering the collision chamber, with the typical current of 200 pA during the coincidence measurement. The vacuum is better than  $10^{-9}$  mbar in the beam line. In order to reduce the contamination from the collisions between the primary beam and the residual gas, several sets of electrostatic deflectors are installed in front of the collision zone to clean the beam. The chamber pressure used in measurement is

$8.5 \times 10^{-8}$  mbar with the driving pressure of 2 bars. The density of gas target is about  $5 \times 10^{11}$  atoms/cm<sup>2</sup>. The ion beam intersects with a supersonic argon gas jet at a right angle in the center of the time-of-flight (TOF) spectrometer. A weak electrostatic field of 1.8 V/cm perpendicular to the ion beam and the gas jet is used to extract the recoil ions and electrons from the collision area in opposite directions. A homogeneous magnetic field (10 Gs) parallel to the electric field forces the electrons to move in spiral trajectories from the reaction volume to the detector. Positions of the recoil ions and electrons are recorded by two two-dimensional position-sensitive detectors placed on opposite ends of the extraction region. The geometry of the accelerating tube and drifting tube of the TOF spectrometer meets the time focusing condition to reduce the momentum broadening caused by the target spread [34]. The projectiles with different charge states are analyzed by an electrostatic deflector downstream of the collision center and the primary beam is directed to a Faraday cup while the charged changed projectiles via electron capture are directed to a position-sensitive MCP detector and give trigger signals. Based on the time of flight, the charge state and the momentum of the recoil ion in the field direction can be obtained; two other components perpendicular to the field direction can be calculated from the flight time and the position on the recoil detector. The electron momentum can be reconstructed according to the same principle as that for the recoil ion. The electron energy resolution varies with its kinematic energy; for

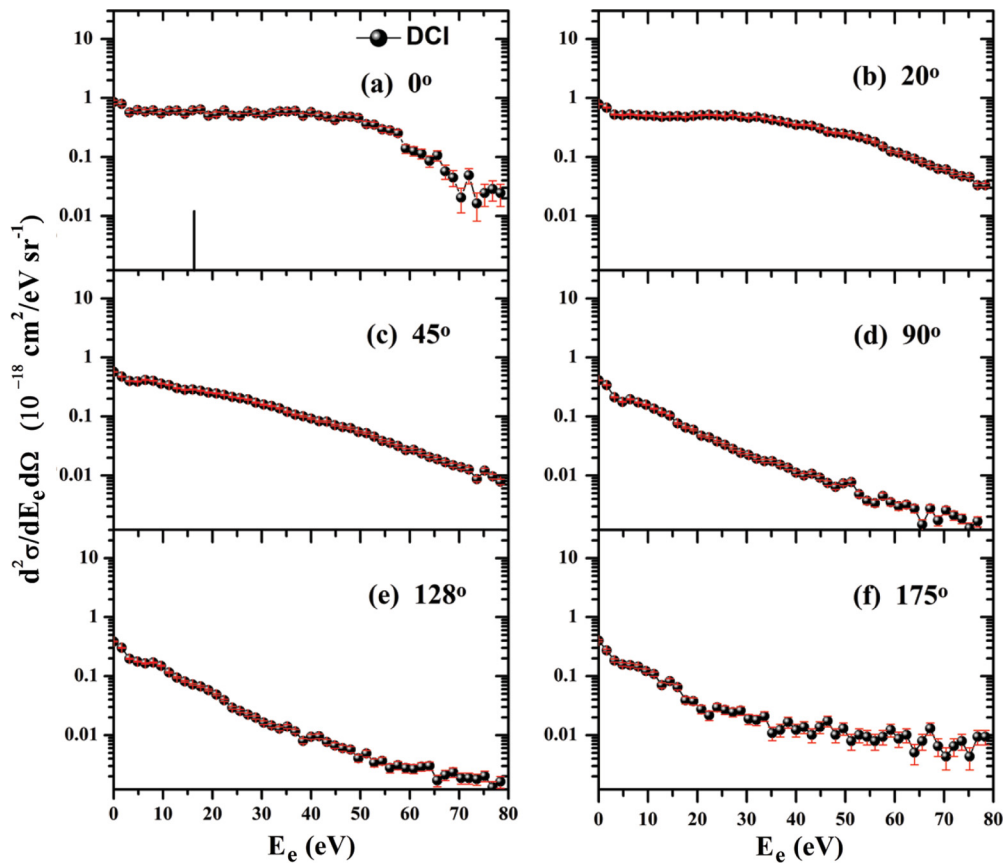


FIG. 1. (Color online) Double-differential cross sections of electrons ejected in the DCI process of the 30 keV/u  $\text{He}^{2+}$  on Ar collision, for electron emission angles of (a)  $\theta = 0^\circ$ , (b)  $\theta = 20^\circ$ , (c)  $\theta = 45^\circ$ , (d)  $\theta = 90^\circ$ , (e)  $\theta = 128^\circ$ , and (f)  $\theta = 175^\circ$ . Lines are to guide the eyes. The short vertical line in (a) indicates the expected position of the cusp peak.

example, the estimated energy resolution is better than 0.3 eV for electron energy less than 1 eV and approximately 1.5 eV for electron energy equal to 16 eV. The momentum resolution of the recoil ions and electrons for the spectrometer has been investigated in detail [35], taking the He target as an example. The resolution of recoil ion momentum is mainly determined by the thermal motion of target atoms and the broadness of the target. In our case, for example, the resolution of the parallel and perpendicular momentum component with respect to the electrostatic field of the TOF spectrometer at a momentum of 2 a.u. is 0.03 a.u. and 0.25 a.u., respectively.

In the present experiment, triple coincidence measurement between the recoil ions, outgoing projectiles, and emitted electrons was carried out. From the two-dimensional spectrum of the recoil ion flight time versus the scattered ion position, at least seven transfer ionization reaction channels are identified [33,36]. In the present paper, we select the double capture with simultaneous single ionization reaction channel. The absolute cross section values are obtained by integrating the measured counts of differential cross sections and normalizing to the value of total cross sections reported by Dubois [37], and only the statistical errors are presented.

In Fig. 1, the DDCSs of the emitted electrons as a function of the electron energy for emission angles of  $0^\circ$ ,  $20^\circ$ ,  $45^\circ$ ,  $90^\circ$ ,  $128^\circ$ , and  $175^\circ$  are presented for the DCI process. For emission angles less than  $20^\circ$ , the spectra have similar features, i.e., the DDCS is nearly flat for electrons with energies less than about 50 eV and then rapidly decreases. However, for emission angles greater than  $20^\circ$ , the DDCS decreases as the electron energy increases, and for larger emission angles, the decrease is faster. In Fig. 1(a), we mark the cusp electron position with a short vertical line, where the electron energy is 16.3 eV. It is observed that there is no cusp-shaped peak in the energy spectrum for the emission angle of  $0^\circ$ . This observation is contrary to the earlier experimental results reported by Fregenal *et al.* [32].

In the experiment performed by Fregenal, an effusive argon target was used and the pressure in the transport line and the working pressure in the collision chamber were  $2 \times 10^{-7}$  and  $1 \times 10^{-6}$  Torr, respectively. Under these vacuum conditions, multiple collisions were unavoidable in the experiment. There can be two main contamination sources that contribute to false coincidences in Fregenal's experiment. The first possibility is the consecutive single collisions between the incident  $\text{He}^{2+}$  ions and two individual target atoms. It should be noted that two cases of the contamination due to the double collisions might be important. The first case is the double capture of the  $\text{He}^{2+}$  collision with one argon atom and single ionization (SI) of another argon atom caused by neutralized He; the second case is that one electron is transferred and one electron is ionized simultaneously (TIII) in the first collision of  $\text{He}^{2+}$  on argon atom and single capture (SC) in the second collision of  $\text{He}^+$  on Ar. Because the cross sections of each collision are large compared to those of the DCI [32], a double coincidence between the outgoing projectile and the emitted electron can result in the observation of cusp-shaped electron emission, which is actually produced in the SI or TIII. A second source of the undesired coincidences arises from the ionization of Ar by the impact of the neutral He, which is neutralized in the beam path through the interaction with residual gas. In

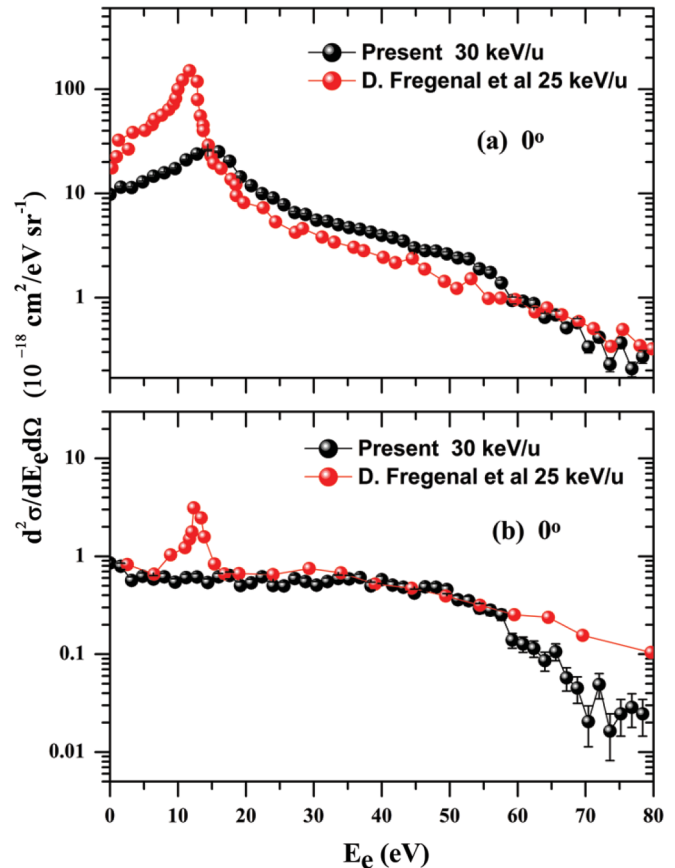


FIG. 2. (Color online) Comparison of DDCS at the emission angle of  $0^\circ$  between the experiment of Fregenal *et al.* [32] and the present experiment. DDCS of total electron emission, (b) DDCS of DCI process. The red (gray) dots and the black dots represent the results of Fregenal *et al.* and our results, respectively. The observed differences in the 60–80-eV range are due to incomplete collection of the electrons at energies larger than 60 eV in the present experiment.

our experiment, the vacuum in the transport line is nearly two orders of magnitude better than that of Fregenal; this advantage reduces the contamination from the latter case to a negligible amount.

A comparison between the results of Fregenal *et al.* and the present results is shown in Fig. 2. In the present analysis of the cusp electron emission, the half angle of the acceptance cone was chosen to be  $3^\circ$ , while it was  $2^\circ$  in the work of Fregenal *et al.* [32]. The presence of the cusp in the spectrum of the total electron emission (TEE) obtained in the present work [Fig. 2(a)] proves that our experimental conditions were suitable for the measurement of the cusp. At the same time, as shown in Fig. 2(b) there is a significant difference for the cusp-shaped electron emission in the DCI channel between the result of Fregenal *et al.* and the present result; the cusp peak is completely missing in the spectrum measured in the present work.

Qualitatively, it would make sense to draw an analogy between the cusp formation in the DCI process and the ionization of the atom by the impact of a neutral projectile. In the latter case, the formation of the cusp peak can be considered as an elastic scattering between the electrons with

extremely low energy relative to the projectile and outgoing projectile. Within the framework of the general FSI theory [27], the DDCS is enhanced by a factor that can be expressed as follows:  $F(v') \propto a^2/(1 + a^2v'^2)$ , where  $a$  is the  $s$ -wave scattering length, and  $v'$  is the electron velocity in the projectile frame. Macri and Barrachina evaluated the enhancement factor for the ground state  $1^1S$  and the metastable states  $2^1S$  and  $2^3S$  of helium [38,39]. It has been shown that the enhancement factor exhibits a giant increase at small energies for the  $e+\text{He}$  ( $2^1S$ ) interaction. This sharp effect is caused by the presence of a low-lying virtual state with a scattering length of approximately  $a = -330$  a.u. [40]. The enhancement factor for the  $e+\text{He}$  ( $2^3S$ ) interaction indicates much more moderate behavior. However, for the  $e+\text{He}$  ( $1^1S$ ) interaction, the sharp effect is not expected. Therefore, the cusp-shaped electron emission was mainly caused by the contribution of the metastable He. Furthermore, the formation of the cusp shape depends significantly on the electronic configurations of the neutral outgoing projectile. If the neutral outgoing projectile were in an excited state, the cusp peak would occur; if the neutral outgoing projectile were in the ground state, the cusp peak would not be expected.

Since the electronic configurations of the outgoing projectile significantly determine the occurrence of the cusp-shaped peak, it is essential to obtain the relative importance of the two electrons captured into the ground state and the excited states of He in the transfer ionization process. Due to the poor resolution of the recoil longitudinal momentum, it is difficult to distinguish the final states of the projectile in the ground state or in an excited state in the present experiment. However, Moretto-Capelle *et al.* have provided the energy potential curve with respect to the different entrance and exit channels in the  $\text{He}^{2+}$  and argon collisions. It is suggested that only 5 eV of energy is required from the internuclear motion to populate the  $\text{He}(1s^2) + \text{Ar}^{3+}$  channel, while much more energy is needed for the  $\text{He}(1snl, n > 2) + \text{Ar}^{3+}$  channel [31]. It can be argued that the  $\text{He}(1s^2) + \text{Ar}^{3+}$  channel will be favored because of the energy proximity in the energy curve diagram. Therefore, the possibility of the cusp-shaped electron formation for the  $\text{He}(1s^2) + \text{Ar}^{3+}$  final state should not be expected.

The broad energy range from 0 to 50 eV in the DDCS at the emission angle of  $0^\circ$  should be noted; this phenomenon would reflect the fact that a considerable amount of electrons

result from the ionization of  $\text{Ar}^{2+}$ , because the larger binding energy leads to broader energy distribution. For the DDCS at the angle of  $20^\circ$ , a plateau of 5–40 eV is also observed. For the electrons ejected with low energies (0–2 eV) in the DCI, the DDCSs at the angles of  $0^\circ$ ,  $20^\circ$ ,  $45^\circ$ ,  $90^\circ$ ,  $128^\circ$ , and  $175^\circ$  are not drastically changed. This result is similar to the result in single ionization, in which the cross sections of the low-energy electron emissions are independent of the emission angles [41] because the yield of the low-energy electrons is strongly affected by the target-center effects. However, the experimental cross sections of the low-energy electrons are significantly deviated from the values predicted by the Born approximation. This result can be clarified by the more suitable theories involving prior and postcollision effects, such as Continuum Distorted Wave Eikonal Initial State approximation (CDW-EIS) [42].

In conclusion, a kinematically complete experiment of the 30 keV/u  $\text{He}^{2+}$  and argon collision have been performed using the reaction microscope. The DDCSs are obtained as a function of the ejected electron energy for different emission angles in the DCI process. The cusp-shaped peak in the forward electron emission is not observed. We investigated this phenomenon by comparing the cusp formation in the present DCI process to that in the ionization of the atom impacted by the neutral projectile. Previous results have suggested that double electrons are primarily captured into the ground state of He in the DCI process of  $\text{He}^{2+}$  on argon collisions at low impact energies. Furthermore, it is emphasized that the cusp peak would not clearly appear when double electrons are captured into the ground states of He within the framework of the FSI theory. Additionally, these results indicated that the cusp peak is not expected in the present reaction channel. Finally, we provided an explanation addressing why the cusp peak does not exist in the present DCI process.

This work is supported by the Major State Basic Research Development Program of China (973 Program, Grant No. 2010CB832902) by the National Natural Science Foundation of China under Grants No. 10979007 and No. 10974207, and by HCJRG-108. This work was partially supported by Helmholtz Alliance EMMI. We would like to thank the engineers who operated the 320-kV platform for their assistance in running the ECR ion source.

- 
- [1] M. E. Rudd and J. Macek, *Case Stud. At. Phys.* **3**, 125 (1972).  
 [2] M. W. Lucas and K. G. Harrison, *J. Phys. B: At. Mol. Phys.* **5**, L20 (1972).  
 [3] W. Oswald, R. Schramm, and H. D. Betz, *Phys. Rev. Lett.* **62**, 1114 (1989).  
 [4] R. G. Pregliasco, C. R. Garibotti, and R. O. Barrachina, *J. Phys. B: At. Mol. Phys.* **27**, 1151 (1994).  
 [5] D. H. Lee, P. Richard, T. J. M. Zouros, J. M. Sanders, J. L. Shynpaugh, and H. Hidmi, *Phys. Rev. A* **41**, 4816 (1990).  
 [6] Y. D. Wang, V. D. Rodríguez, C. D. Lin, C. L. Cocke, S. Kravis, M. Abdallah, and R. Dörner, *Phys. Rev. A* **53**, 3278 (1996).  
 [7] R. E. Olson and A. Salop, *Phys. Rev. A* **16**, 531 (1977).  
 [8] G. B. Crooks and M. E. Rudd, *Phys. Rev. Lett.* **25**, 1599 (1970).  
 [9] A. Salin, *J. Phys. B: At. Mol. Phys.* **5**, 979 (1972).  
 [10] K. Dettmann, K. G. Harrison, and M. W. Lucas, *J. Phys. B: At. Mol. Phys.* **7**, 269 (1974).  
 [11] J. Briggs, *J. Phys. B: At. Mol. Phys.* **10**, 3075 (1977).  
 [12] D. S. F. Crothers and J. F. McCann, *J. Phys. B: At. Mol. Phys.* **16**, 3229 (1983).  
 [13] P. D. Fainstein, V. H. Ponce, and R. D. Rivarola, *J. Phys. B: At. Mol. Phys.* **21**, 287 (1988).  
 [14] J. Ullrich, R. Moshhammer, A. Dorn, R. Dörner, L. Ph. H. Schmidt, and H. Schimidt-Böcking, *Rep. Prog. Phys.* **66**, 1463 (2003).

- [15] R. Dörner, V. Mergel, O. Jagutzki, L. Spielberger, J. Ullrich, R. Moshhammer, and H. Schmidt-Böcking, *Phys. Rep.* **330**, 95 (2000).
- [16] V. Mergel, R. Dörner, K. Khayyat, M. Achler, T. Weber, O. Jagutzki, H. J. Lüdde, C. L. Cocke, and H. Schmidt-Böcking, *Phys. Rev. Lett.* **86**, 2257 (2001).
- [17] V. Mergel, R. Dörner, M. Achler, Kh. Khayyat, S. Lencinas, J. Euler, O. Jagutzki, S. Nüttgens, M. Unverzagt, L. Spielberger, W. Wu, R. Ali, J. Ullrich, H. Cederquist, A. Salin, C. J. Wood, R. E. Olson, Dž. Belkić, C. L. Cocke, and H. Schmidt-Böcking, *Phys. Rev. Lett.* **79**, 387 (1997).
- [18] M. Schulz, D. Fischer, R. Moshhammer, and J. Ullrich, *J. Phys. B: At. Mol. Phys.* **38**, 1363 (2005).
- [19] P. A. Závodszky, L. Sarkadi, J. A. Tanis, D. Berényi, J. Pálinkás, V. L. Plano, L. Gulyás, E. Takács, and L. Tóth, *Nucl. Instrum. Methods Phys. Res., Sect. B* **79**, 67 (1993).
- [20] M. Zhu, R. R. Haar, S. M. Ferguson, O. Voitke, J. A. Tanis, L. Sarkadi, J. Pálinkás, P. A. Závodszky, and D. Berényi, *Nucl. Instrum. Methods Phys. Res., Sect. B* **98**, 351 (1995).
- [21] L. Víkor, P. A. Závodszky, L. Sarkadi, J. A. Tanis, M. Kuzel, A. Bader, J. Pálinkás, E. Y. Kamber, D. Berényi, and K. O. Groeneveld, *J. Phys. B: At. Mol. Phys.* **28**, 3915 (1995); L. Víkor, L. Sarkadi, J. A. Tanis, A. Báder, P. A. Závodszky, M. Kuzel, K. O. Groeneveld, and D. Berényi, *Nucl. Instrum. Methods Phys. Res., Sect. B* **124**, 342 (1997).
- [22] L. V. Plano, R. R. Haar, J. A. Tanis, J. Pálinkás, L. Sarkadi, P. A. Závodszky, D. Berényi, H. Khemliche, M. H. Prior, and D. Schneider, *Nucl. Instrum. Methods Phys. Res., Sect. B* **86**, 181 (1994).
- [23] J. H. McGuire, T. Reeves, N. C. Deb, and N. C. Sil, *Nucl. Instrum. Methods Phys. Res., Sect. B* **24**, 243 (1987).
- [24] L. Sarkadi, J. Pálinkás, A. Kövér, D. Berényi, and T. Vajnai, *Phys. Rev. Lett.* **62**, 527 (1989).
- [25] A. Salin, *Nucl. Instrum. Methods Phys. Res., Sect. B* **86**, 1 (1994).
- [26] L. Szótér, *Phys. Rev. Lett.* **64**, 2835 (1990).
- [27] R. O. Barrachina, *J. Phys. B: At. Mol. Phys.* **23**, 2321 (1990).
- [28] A. Báder, L. Sarkadi, L. Víkor, M. Kuzel, P. A. Závodszky, T. Jalowy, K. O. Groeneveld, P. A. Macri, and R. O. Barrachina, *Phys. Rev. A* **55**, R14 (1997).
- [29] P. Focke, G. Bernardi, D. Fregenal, R. O. Barrachina, and W. Meckbach, *J. Phys. B: At. Mol. Phys.* **31**, 289 (1998).
- [30] G. Bernardi, P. Focke, A. D. González, S. Suárez, and D. Fregenal, *J. Phys. B: At. Mol. Phys.* **32**, L451 (1999).
- [31] P. Moretto-Capelle, D. Bordenave-Montesquieu, A. Bordenave-Montesquieu, and M. Benhenni, *J. Phys. B: At. Mol. Phys.* **31**, L423 (1998).
- [32] D. Fregenal, J. Fiol, G. Bernardi, S. Suárez, P. Focke, A. D. González, A. Muthig, T. Jalowy, K. O. Groeneveld, and H. Luna, *Phys. Rev. A* **62**, 012703 (2000).
- [33] X. Ma, R. T. Zhang, S. F. Zhang, X. L. Zhu, W. T. Feng, D. L. Guo, B. Li, H. P. Liu, C. Y. Li, J. G. Wang, S. C. Yan, P. J. Zhang, and Q. Wang, *Phys. Rev. A* **83**, 052707 (2011).
- [34] W. C. Wiley and I. H. McLaren, *Rev. Sci. Instrum.* **26**, 1150 (1955).
- [35] D. L. Guo, X. Ma, W. T. Feng, S. F. Zhang, and X. L. Zhu, *Acta Phys. Sin.* **60**, 113401 (2011).
- [36] R. T. Zhang, X. Ma, S. F. Zhang, X. L. Zhu, S. Akula, D. H. Madison, B. Li, D. B. Qian, W. T. Feng, D. L. Guo, H. P. Liu, S. C. Yan, P. J. Zhang, S. Xu, and X. M. Chen, *Phys. Rev. A* **87**, 012701 (2013).
- [37] R. D. DuBois, *Phys. Rev. A* **36**, 2585 (1987).
- [38] R. O. Barrachina, *Nucl. Instrum. Methods Phys. Res., Sect. B* **124**, 198 (1997).
- [39] P. A. Macri and R. O. Barrachina, *J. Phys. B: At. Mol. Phys.* **31**, 1303 (1998).
- [40] R. K. Nesbet, *Phys. Rev. A* **20**, 58 (1979); *J. Phys. B: At. Mol. Phys.* **3**, L193 (1980).
- [41] N. Stolterfoht, R. D. DuBois, and R. D. Rivarola, *Electron Emission in Heavy Ion-Atom Collisions* (Springer, Berlin, 1997).
- [42] J. M. Monti, O. A. Fojón, J. Hanssen, and R. D. Rivarola, *J. Phys. B: At. Mol. Phys.* **46**, 145201 (2013).